Development of a New Cfd-Based Unified Closure Relation for Taylor Bubble Velocity in Two-Phase Slug Flow in Pipes

BHR Group
EXPERTS IN FLUID ENGINEERING

Development of a new CFD-based unified closure relation for Taylor bubble velocity in two-phase slug flow in pipes

E. Lizarraga-Garcia[1], J. Buongiorno[2,3], E. Al-Safran[4] and D. Lakehal[5]

[1]Department of Mechanical Engineering, MIT, Cambridge, USA
[2]Department of Nuclear Science and Engineering, MIT, Cambridge, USA
[3]Corresponding author, jacopo@mit.edu
[4]Department of Petroleum Engineering, Kuwait University, Kuwait
[5]ASCOMP, Zurich, Switzerland

ABSTRACT

Two-phase slug flow is a common occurrence in wells, riser pipes and pipelines of crude oil and natural gas systems. Current predictive tools for two-phase flow are based on either the mixture model or the mechanistic two-fluid model. The latter one, also called phenomenological model, requires the use of closure relations to solve the transfer of mass, momentum and energy between the phases, in the respective conservation equations, so that integral flow parameters such as liquid holdup (or void fraction) and pressure gradient can be predicted. However, these closure relations carry the highest uncertainties in the model, since they are obtained empirically or through the use of overly simplified assumptions. In particular, significant discrepancies have been found between experimental data and closure relations for the Taylor bubble velocity in slug flow, which has been determined through an in-house study to strongly affect the pressure gradient and liquid holdup predicted by the mechanistic models of (Orell and Rembrand, 1986), (Ansari et al., 1994), and (Petalas and Aziz, 2000). In this work, Computational Fluid Dynamics (CFD) and the Level Set (LS) interface tracking method (ITM), implemented in the commercial code TransAT®, are employed to simulate the motion of Taylor bubbles in slug flow. Therefore, a numerical database is being generated to develop a new, high-fidelity closure relation for the Taylor bubble velocity as a function of the fluid properties and flow conditions, rendered non-dimensional through the use of the Froude, Reynolds, Eötvös and Morton numbers, and pipe inclination angle. The simulations suggest that in inclined pipes the Taylor bubble velocity is strongly reduced if there is no lubricating liquid film between the bubble and the wall. A simple analytical model predicting the drainage of this lubricating film is also presented.

1 INTRODUCTION

Two-phase slug flow is a common occurrence in wells, riser pipes and pipelines of crude oil and natural gas systems. Current predictive tools for two-phase flow are based on either the mixture model or the mechanistic two-fluid model (Brill and Mukherjee, 1999). In the latter one, slug flow is modeled as a sequence of fundamental units, also called slug units. Each unit contains a long bullet-shaped bubble, known as Taylor bubble, and a liquid portion with smaller homogeneously distributed bubbles, known as liquid slug. This model requires the use of closure relations to solve the transfer of mass, momentum and energy between the phases, in the respective conservation equations, so that integral flow parameters such as liquid holdup (or void fraction) and pressure gradient can be predicted. However, these closure relations carry the highest uncertainties in the model, since they are obtained empirically or through the use of overly simplified assumptions. In particular, significant discrepancies have been found between experimental data and closure relations for the Taylor bubble velocity in slug flow, which has been determined through an in-house study to strongly affect the pressure gradient and liquid holdup predicted by the mechanistic models of Ansari et al. (1994), Orell and Rembrand (1986), and Petalas and Aziz (2000).

Thorough studies about the modeling of two-phase slug flow can be found in Bendiksen et al. (1996), Fabre and Liné (1992), and Taitel and Barnea (1990). Taylor bubble's dynamics are influenced by the viscous, inertial, gravitational, and interfacial forces acting on it. Dimensional analysis leads to the following dimensional groups:

$$u_{TB}\Big/\sqrt{gd\frac{(\rho_L-\rho_g)}{\rho_L}};\ \frac{g(\rho_L-\rho_g)d^2}{\sigma};\ \frac{g\mu_L^4(\rho_L-\rho_g)}{\rho_L^2\sigma^3};\frac{\rho_L u_L d}{\mu_L};\ \frac{\rho_g}{\rho_L};\ \frac{\mu_g}{\mu_L};\frac{L_{TB}}{d};\theta;$$

where u_{TB} is the Taylor bubble velocity, g is the gravity, d is the pipe diameter, ρ_L is the liquid density, ρ_g is the gas density, σ is the surface tension, μ_L is the liquid viscosity density, u_L is the average inlet liquid velocity, μ_g is the gas viscosity, L_{TB} is the Taylor bubble length, and θ is the inclination angle with respect to the horizontal. For vertical circular tubes, the film thickness and the Taylor bubble velocity are independent of the bubble length (Griffith and Wallis, 1961; Llewellin et al., 2012; Mao and Dukler, 1989; Nicklin et al., 1962; Tomiyama et al., 2001). Moreover, it has been observed that Taylor bubble velocity is also independent of its length for inclined pipes (see Section 2.2.2). The density and viscosity are much lower in the gas than in the liquid $\left(\rho_g/\rho_L \ll 1, \mu_g/\mu_L \ll 1\right)$ and over the range of conditions of interest it can be assumed that the Taylor bubble velocity will not depend on the density and viscosity ratios. Thus, only five non-dimensional numbers (or Pi groups) describe the motion of a Taylor bubble in a circular tube. Using the previous approximations, these are the Froude number $Fr = u_{TB}/\sqrt{gd}$, which is the ratio of the bubble inertia to the gravitational forces; the Eötvös number $Eo = g\rho_L d^2/\sigma$, which is the ratio of the gravitational to interfacial forces; the Morton number $Mo = g\mu_L^4/\rho_L\sigma^3$, sometimes called the property group; the liquid Reynolds number $Re_L = \rho_L u_L d/\mu_L$, which is the ratio of the inertial to viscous forces in the liquid phase, and θ. Thus, Buckingham Pi Theorem assures that the five Pi groups are related by a unique function of the form $Fr = f(Eo, Mo, Re_L, \theta)$. Finding this function is the ultimate objective of this study. Note, however, that the choice of Pi groups is not unique; for example, the inverse viscosity number $N_f = \rho_L\sqrt{gd^3}/\mu_L$, which is a combination of the Eötvös and Morton numbers, $N_f = (Eo^3/Mo)^{1/4}$; the Archimedes number $Ar = \sigma^{3/2}\rho_L^{1/2}/\mu_L^2 g^{1/2}$, which is $Ar = (1/Mo)^{1/2}$; the capillary

number, $Ca = Fr(Eo \cdot Mo)^{1/4}$; or the Weber number, $We = Fr^2 \cdot Eo$, are often also used.

The literature for Taylor bubbles moving in vertical tubes ($\theta = 90°$) filled with stagnant liquid ($Re = 0$) is extensive. Davies and Taylor (1950), and Dumitrescu (1943) studied analytically the limiting problem of negligible viscous force and surface tension where Fr is constant. White and Beardmore (1962) performed a wide range of experiments for vertical tubes of stagnant liquid and proposed a general graphical correlation of Fr as a function of Eo and Mo identifying regions where some governing forces can be neglected (see Figure 1). Furthermore, empirical correlations for this case are given by Viana et al. (2003), Wallis (1969), and Zukoski (1966). The motion of Taylor bubble in liquid flow, that is $Re \neq 0$, is more complex. Taylor bubble velocity in two-phase flow is modeled based on the approach of Nicklin et al. (1962),

$$\boldsymbol{u_{TB} = C_0 u_m + u_d}, \qquad (1)$$

where u_d is the drift velocity of the bubble in stagnant liquid, and $C_0 u_m$ is the contribution of the mixture velocity u_m which is the sum of the liquid and gas superficial velocities $u_m = u_{SL} + u_{Sg}$, respectively. The coefficient C_0 is a dimensionless coefficient that depends on the velocity profile above the bubble, and is approximately the ratio of the maximum to the mean profile velocity. Thus, for vertical pipes it is usually accepted as a good engineering approximation that $C_0 \sim 2$ for laminar flow in round pipes, and $C_0 \sim 1{,}2$ for turbulent flow in round pipes, which is reinforced by experiments (Bendiksen, 1984; Nicklin et al., 1962; Polonsky et al., 1999) and theory (Collins et al., 1978). For the case of a single Taylor bubble inside flowing liquid, the model of Nicklin et al. (1962) states that $u_{TB} = C_0 u_{SL} + u_d$. Expressions for the coefficient C_0 are found in the literature: for example, for vertical flow, there are expressions of C_0 as a function of Re_L only (Fréchou, 1986), and of Re_L and Eo (Bendiksen, 1984; Tomiyama et al., 2001). Also, Petalas and Aziz (2000) used in their mechanistic model an expression of C_0 for inclined pipes that depends on Re_L and θ. Numerical simulations by Mao and Dukler (1991) matched well with the correlation of Fréchou (1986). The motion of Taylor bubbles in inclined pipes has also been studied in the literature. For example, Zukoski (1966) investigated experimentally the influence of liquid viscosity and surface tension on the bubble velocity, proposing a velocity correlation for vertical tubes, and describing qualitatively the effect of tube inclination in closed tubes. Bendiksen (1984) was the first to propose a correlation for inclined pipes,

$$\boldsymbol{u_d = u_d^h \cos\theta + u_d^v \sin\theta}, \qquad (2)$$

where u_d^h and u_d^v are the horizontal and vertical drift velocity, respectively. He claimed that u_d^h is different from zero in some cases: he assumed a system with one pipe end opened and partially filled with liquid and gas where liquid leaves and gas enters moving the bubble forward inside the pipe due to the liquid level differences at both sides of the Taylor bubble. This contradicted previous investigations such as Dukler and Hubbard (1975), and Nicklin et al. (1962) who assumed $u_d^h = 0$ in a closed horizontal pipe. Weber et al. (1986) proposed another experimental correlation for Fr_d in closed and inclined pipes based on the horizontal and vertical Froude numbers Fr_d^h and Fr_d^v, respectively, and θ, with an extra correction term different from Bendiksen's correlation. Hasan and Kabir (1988) proposed a new experimental correlation for $30° < \theta < 90°$ based on θ and u_d^v only, assuming $u_d^h = 0$. Jeyachandra et al. (2012) analyzed experimentally the Taylor bubble terminal velocity for high-viscosity oil and slightly modified Bendiksen's

correlation. Carew et al. (1995) derived a semi-theoretical expression for the rise velocity of air bubbles in inclined pipes of stagnant water. Other experimental studies of inclined or slightly inclined tubes of stagnant liquid have been carried out by Alves et al. (1993), Bonnecaze et al. (1971), Shosho and Ryan (2001), Spedding and Nguyen (1978), and Stanislav et al. (1986).

CFD numerical simulations have also been used to study slug flow. Clarke and Issa (1997), and Mao and Dukler (1990) focused on the flow ahead and around the bubble. Araújo et al. (2012) provided a wide range of Taylor bubbles in vertical columns of stagnant liquid using 2D axisymmetric simulations. Araújo et al. (2013a) and Araújo et al. (2013b) studied the hydrodynamics of pairs of consecutive Taylor bubbles in stagnant and flowing liquid, respectively. Other 2D vertical axisymmetric studies were done by Bugg et al. (1998), and Kang et al. (2010). Taha and Cui (2006) went further and performed some 3D inclined pipe simulations. Lakehal et al. (2012) and Caviezel et al. (2013) presented "*proof of concept*" 3D resolved-interface simulations of Taylor bubbles in vertical riser flow (reduced length), and reached the conclusion that ITM techniques cannot resolve the cloud of small bubbles generated in the wake of the Taylor bubble, and need therefore to be coupled with phase-average methods. Furthermore, Lakehal et al. (2011) performed 3D simulations to study the transition of gas-liquid stratified flow to slug flow in horizontal pipes, where the previously mentioned coefficient C_0 is also analyzed. Our current project's goal is to thoroughly study the inclination effect on the Taylor bubble dynamics, including its velocity, through 3D CFD simulations with ITM. PIV experimental data is very useful for code validation: Bugg and Saad (2002) provided such data for a vertical pipe of stagnant viscous liquid. Nogueira et al. (2006a), and Nogueira et al. (2006b) studied the nose region and annular film, and the wake of Taylor bubbles, respectively, in vertical pipes of stagnant and flowing liquids. Liu et al. (2013) analyzed the wake structure of Taylor bubbles in liquid nitrogen in inclined pipes.

A general theory for the Taylor bubble velocity in inclined pipes is currently lacking. Herein, a number of 3D numerical simulations of Taylor bubble motion in stagnant liquid for a wide range of liquid properties, pipe diameters and inclinations is presented. Successful preliminary simulations of Taylor bubbles in flowing liquid have also been performed, although they are not included in this article.

2 CFD SIMULATIONS

3-D CFD simulations have been performed with the CMFD code TransAT® (TransAT®, 2014), a finite-volume software developed at ASCOMP. The code uses structured meshes and MPI parallel-based algorithm to solve multi-fluid Navier-Stokes equations. Computer resources for this work include the supercomputers Titan and Eos of the Oak Ridge Leadership Computing Facility at the Oak Ridge National Laboratory.

2.1 Mathematical model

TransAT® uses the one-fluid formulation approach, where the flow is described by one fluid with variable material properties, which vary according to a color function, which is advected by the flow, thus identifying the gas and liquid regions. In the absence of phase change phenomena, the mass and momentum conservation equations are

$$\frac{\partial \boldsymbol{\rho}}{\partial \boldsymbol{t}} + \boldsymbol{\nabla} \cdot (\boldsymbol{\rho u}) = \mathbf{0}, \qquad (3)$$

$$\frac{\partial(\rho \boldsymbol{u})}{\partial t} + \nabla \cdot (\rho \boldsymbol{u}\boldsymbol{u}) = -\nabla p + \nabla \cdot \boldsymbol{\sigma} + \rho \boldsymbol{g} + \boldsymbol{F}_s, \quad (4)$$

where t is the time, ρ is the density, $\boldsymbol{u}$ is the velocity vector, p is the pressure, $\boldsymbol{\sigma} = \mu(\nabla \boldsymbol{u} + \nabla^T \boldsymbol{u})$ is the viscous stress tensor where μ is the viscosity, $\boldsymbol{g}$ is the gravity vector, and $\boldsymbol{F}_s = \gamma \kappa \boldsymbol{n} \delta(\phi)$ is the surface tension term where γ is the surface tension coefficient, $\kappa = -\nabla \phi / |\nabla \phi|$ is the surface curvature, $\boldsymbol{n}$ is the vector normal to the interface, and δ is a smoothed delta function centered at the interface. In this work, the color function used is based on the Level Set (LS) method (Osher and Sethian, 1988), where the interface is represented by a continuous and monotonous function ϕ that represents the distance to the interface at which $\phi = 0$. The LS advection equation is given by

$$\frac{\partial \phi}{\partial t} + \boldsymbol{u} \cdot \nabla \phi = \boldsymbol{0}, \quad (5)$$

and material properties such as density and viscosity are updated locally based on ϕ, and smoothed across the interface using a smooth Heaviside function. A mass conservation scheme is also employed to avoid scheme-induced losses. Furthermore, the pipe is modeled as an embedded surface and represented in the fluid by the so-called Solid Level Set function where $\phi_s = 0$ is the fluid-solid interface (i.e. the IST technique).

2.2 Results

2.2.1 Vertical pipes

Table 1 shows the test matrix for simulations of Taylor bubble motion in vertical pipes ($\theta = 90°$) with no imposed flow ($Re = 0$) performed with TransAT®, whose cases are localized in the experimental map of White and Beardmore (1962) in Figure 1, where the x-axis is the Eo number, and the y-axis is the Mo number.

Table 1: Test matrix for simulations of Taylor bubble motion in vertical pipes ($\theta = 90°$) with no imposed flow ($Re = 0$).

Case	Mo	Eo	N_f	Fr (lit.)	Fr (sim.)	$\bar{h}$ (lit.)	$\bar{h}$ (sim.)
1	0,328	76,5	34,2	0,210	0,212	0,295	0,288
2	$4{,}03 \cdot 10^{-3}$	187	201	0,324	0,306	0,198	0,189
3	19,2	31,2	6,31	0,0573*	0,0418	0,305	0,292
4	$1{,}17 \cdot 10^{-4}$	38,6	149	0,276*	0,295	0,212	0,234
5	$1{,}52 \cdot 10^{-2}$	98,4	89,0	0,303*	0,291	0,246*	0,238
6	$1{,}50 \cdot 10^{-3}$	9,88	28,3	0,0411	0,0458	0,192	0,189
7	$4{,}75 \cdot 10^{-2}$	192	111	0,336*	0,322	0,235*	0,218
8	8,38	747	84,0	0,289*	0,299	0,250	0,261
9	8,38	181	29,0	0,199	0,216	0,306	0,295
10	$3{,}73 \cdot 10^{-11}$	23,8	4360	0,300*	0,285	0,073	0,102

*: indicates experimental value in the literature columns. Otherwise, the literature values are obtained with correlations.

The numerically obtained Fr number is successfully compared to its values found in the literature. Six cases are compared with experimental data (cases 3 and 4 with Shosho and Ryan (2001); case 5 with Bugg and Saad (2002); case 7 with Nogueira et al. (2006a); case 8 with Jeyachandra et al. (2012); and case 10 with Tomiyama et al. (2001)), whereas the other four cases are compared with the correlation of Viana et al. (2003). The average terminal velocity error of the simulations is -1,4%, with a standard deviation equal to 10.4%. Using the correlation of Viana et al. (2003) for cases 3 and 4 instead of the experimental values of Shosho and Ryan (2001), the error is 0,182+/-6,1%. Figure 2 shows a graphical comparison between the numerical and the literature Fr values of Table 1. Similarly, the developed non-dimensional film thickness $\bar{h} = h/R$, where R is the pipe radius, compares well with data from the literature. Two cases are compared with experimental data (case 5 (Bugg and Saad, 2002); and case 7 (Nogueira et al., 2006a)). The other eight cases are compared with the correlations provided by Llewellin et al. (2012): their so-called Cubic Brown model (equations 2.5 and 2.6 in their article) for cases where the flow in the film is laminar ($N_f \leq 1372$), and an empirical correlation (equation 4.2 in their article) for case 10, where $N_f > 1372$. The Fr needed for these correlations are obtained from the expression of Viana et al. (2003). The average film thickness error of the simulations is 0,457+/-6,26%. Figure 2 shows a graphical comparison between the numerical and the literature $\bar{h}$ values of Table 1.

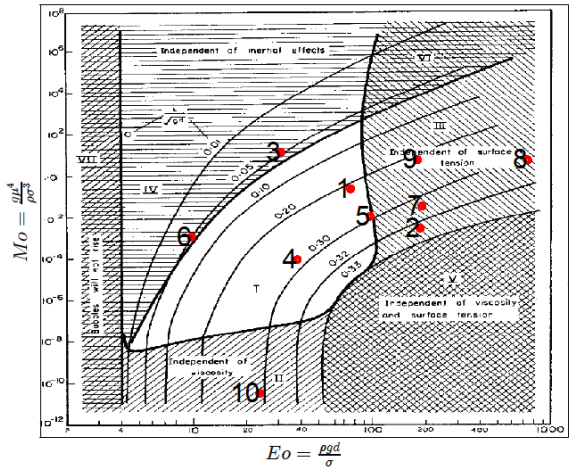

Figure 1: Test matrix for simulations of Taylor bubble motion (see Table 1) localized in the experimental map of White and Beardmore (1962).

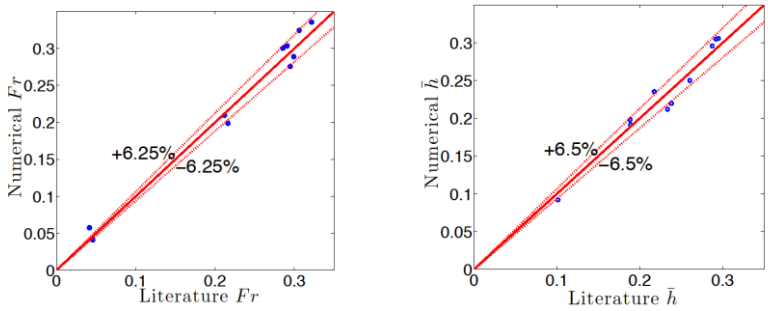

Figure 2: Taylor bubble terminal velocity and film thickness numerical results compared with the literature values.

2.2.2 Inclined pipes

3D CFD simulations of inclined pipes have been performed for cases 1, 3, 4, 8 and 9 from Table 1. The Fr number obtained numerically is compared with the experimental data of Jeyachandra et al. (2012), and Shosho and Ryan (2001), and the correlations from Hasan and Kabir (1988), Jeyachandra et al. (2012), and Petalas and Aziz (2000) in Figure 3 through Figure 5. The correlation of Hasan and Kabir (1988) $Fr_d = Fr_d^v\sqrt{\sin\theta}\,(1+\cos\theta)^{1.2}$, where $Fr_d^v = 0.35$, has been slightly modified so that it also accounts for the surface tension and viscous forces: Fr_d^v is obtained from the correlation of Viana et al. (2003) instead. Hasan and Kabir (1988) assumed that horizontal drift velocity is zero. Furthermore, the vertical velocity of Petalas and Aziz (2000) slug mechanistic model has been calculated using the correct correlation from Wallis (1969). Numerical results compare well with the experimental data. Terminal velocity increases as the pipe inclines. The maximum value results from the competing effects of drag coefficient (lower at lower angles, where most of the liquid "bypasses" the bubble through a larger flow area), and buoyancy (higher at higher angle). Furthermore, successful simulations have been performed down to an inclination angle of 3 degrees for case 4 (Figure 3, right), where a thin film persists between the bubble and the wall and lubricates the bubble motion. The existence of the film is confirmed by the simple analytical drainage model described later in Section 3. As the inclination angle approaches zero, the bubble terminal velocity drops significantly showing a trend towards zero. This would suggest that horizontal drift velocity is zero for a closed tube, although more results are needed to make a conclusive remark on this aspect. Among the correlations used, the one from Hasan and Kabir (1988) captures relatively well the trend of terminal velocity with inclination angle, where the maximum occurs close to the experimental and numerical values in the five cases. However, we think there is room for improvement in the value prediction.

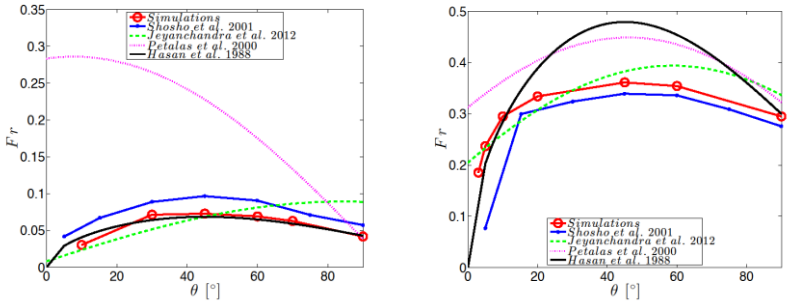

Figure 3: Fr as a function of θ for case 3 (left) and 4 (right) compared with experiments from Shosho and Ryan (2001), and experimental correlations from Hasan and Kabir (1988), Jeyachandra et al. (2012), and Petalas and Aziz (2000).

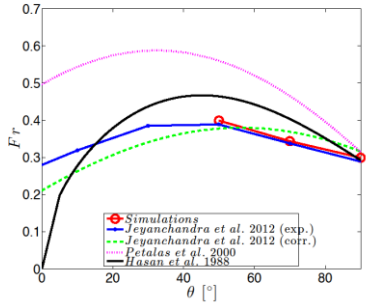

Figure 4: Fr as a function of θ for case 8 compared with experiments from Jeyachandra et al. (2012), and experimental correlations from Hasan and Kabir (1988), Jeyachandra et al. (2012), and Petalas and Aziz (2000).

An interesting question that has not been addressed in the literature yet is the effect of Taylor bubble length on its velocity in inclined pipes. For the vertical case, the bubble velocity is independent of its length (Griffith and Wallis, 1961; Llewellin et al., 2012; Mao and Dukler, 1989; Nicklin et al., 1962; Tomiyama et al., 2001). In the literature, the bubble volume relative to the pipe diameter is represented by the diameter ratio $\lambda = d_e/d$, where d_e is the sphere-volume equivalent diameter of the bubble. When $\lambda > 0{,}6$, bubbles are classified as Taylor bubbles (Tomiyama et al., 2001). Simulations are performed for case 3 for two bubbles of $\lambda = 1{,}17$ and $1{,}05$ for $\theta = 90°$, $60°$ and $45°$. It is found that the terminal velocity is equal for both bubbles for each of the inclination angles. Furthermore, the shape of the bubbles coincides: Figure 6 shows the vertical case (where the film thickness from the correlation of Llewellin et al. (2012) is included), and the two inclined cases.

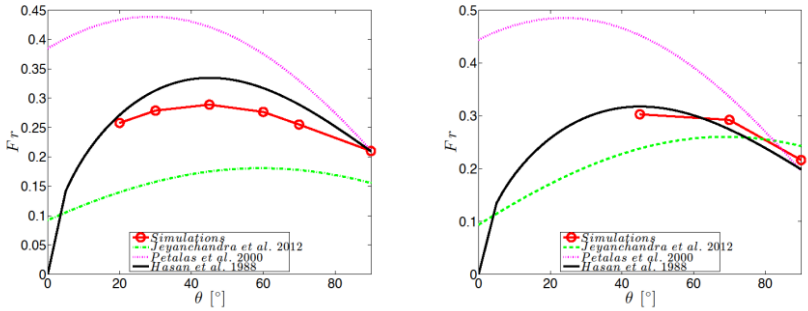

Figure 5: Fr as a function of θ for case 1 (left) and 9 (right) compared with experimental correlations from Hasan and Kabir (1988), Jeyachandra et al. (2012), and Petalas and Aziz (2000).

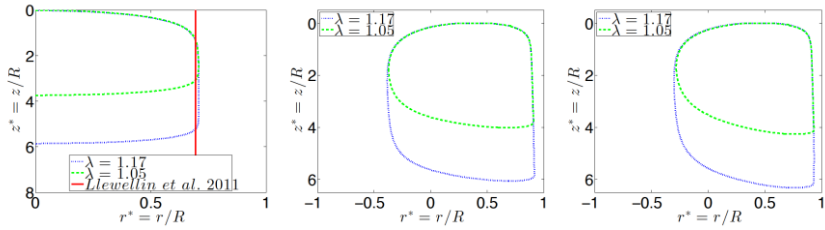

Figure 6: Comparison of the Taylor bubble shape of case 3 for two different bubble volumes of $\lambda = 1,17$ and 1,05 for $\theta = 90°$ (left), $60°$ (middle), and $45°$ (right).

3 FILM BREAKUP CRITERION

For the case of vertical pipes, an axisymmetric lubricating film separates the Taylor bubble from the pipe wall. For stagnant liquid, the range of the non-dimensional film thickness $\bar{h}$ is approximately $\bar{h} \in [0{,}08, 0{,}33]$ (see Llewellin et al. (2012)). As the pipe inclination increases, the Taylor bubble approaches the pipe wall under the effect of buoyancy, and the lubricating film becomes significantly thinner and non-axisymmetric. Moreover, the thickness of the film decreases along the Taylor bubble due to gravity-driven drainage. If the film breaks up, the surface tension force at the triple contact line reduces the velocity of the bubble significantly. The breakup of the film has received some attention in the literature; e.g. Ha-Ngoc and Fabre (2004a), and Maneri and Zuber (1974), where the velocity of plane bubbles in two-dimensional ducts are numerically and experimentally studied, respectively. They observed three different bubble shape regimes depending on the duct inclination; (i) the bubble touches the upper wall for $\theta \leq 60°$, (ii) the lubricating film is stable and the bubble does not touch the duct for $\theta \geq 80°$, and (iii) an unstable transition region in between. Al-Safran et al. (2013) observed a stable thin film at the top of the horizontal pipe in their slug flow experiments with high-viscosity fluids. However, these results are valid for the limited set of fluid properties and flow conditions explored in those studies; a generally-applicable model for the film drainage and breakup cannot be found in the literature. After solving the Navier-Stokes equations for the film with the lubrication approximation, a generally valid drainage and breakup criterion for the lubricating film in slug flow in inclined round pipes has been derived. Figure 7 depicts the film drainage and breakup map, where the y-axis corresponds to the non-dimensional film thickness $\bar{h} = h/h_c$, where h_c is the critical film

thickness at which the film breaks up, and the x-axis corresponds to the non-dimensional time $\bar{t} = t/\tau$, where τ is the characteristic film drainage time based on the fluid properties, pipe geometry, and critical film thickness. As $\bar{t}$ increases, all solutions collapse on one line independent from the initial thickness h_0 due to the fact that an initially thicker film drains faster,

$$\bar{h}(\bar{t}) = \frac{h(\bar{t})}{h_c} = \left(\left(\frac{h_c}{h_0}\right)^2 + \bar{t}\right)^{-1/2}. \qquad (6)$$

Film breakup occurs when $\bar{h} = 1$. However, given the uncertainties in the calculation of the critical film thickness h_c, a conservative assumption is made that film breakup occurs at $\bar{h} = 10$. The intersection between the film drainage curve and $\bar{h} = 10$ occurs at $\bar{t} = 0{,}01$. This time has to be compared to the non-dimensional bubble's passage time $\bar{t}_{bubble}$ through a point in the pipe. Thus, the criterion to avoid film breakup in Taylor flow becomes $\bar{t}_{bubble} < 0{,}01$. Such criterion can be used to determine under what conditions the lubricating film is present, which is a key input for both numerical simulations (Ben-Mansour et al., 2010; Ha-Ngoc and Fabre, 2004b; Taha and Cui, 2006) and mechanistic modeling of slug flow. This criterion has been used in this article's simulations to verify that a lubricating film is present between the Taylor bubble and the wall.

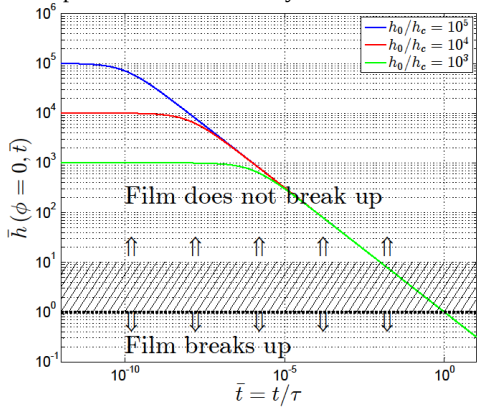

Figure 7: Film drainage and breakup map. The film is conservatively assumed to break if the film thickness decreases to $h < 10h_c$.

4 CONCLUSIONS

The Taylor bubble terminal velocity has been determined through an in-house study to strongly affect the pressure gradient and liquid holdup predicted by the slug flow mechanistic models. This article presents 3D CFD with Level Set simulations performed with the commercial code TransAT® for different liquids in closed tubes. The code is validated through the bubble terminal velocity for different inclination angles, its film thickness for the vertical pipe, and also the liquid velocity vectors. Thus, it is proven this approach's potential to obtain a general expression for the Taylor bubble terminal velocity in inclined pipes, covering the whole range of Newtonian fluids' properties, which is currently lacking in the literature. At this time, a numerical database is being generated to develop a new, high-fidelity closure relation for the Taylor bubble velocity as a function of the fluid properties, flow conditions, and pipe geometry. Furthermore, it is shown that the Taylor bubble length does not affect the terminal velocity in inclined

pipes. Finally, a model predicting the gravity-drainage of the lubricating liquid film between the bubble and the pipe wall in inclined pipes is described, and derived from it a criterion for avoidance of film breakup: $\bar{t}_{bubble} = t_{bubble}/\tau < 0{,}01$, where $\bar{t}_{bubble}$ is the non-dimensional bubble's passage time, and τ is the characteristic film drainage time based on the fluid properties, pipe geometry, and critical film thickness.

5 ACKNOWLEDGEMENTS

Support from the MIT-Kuwait Center for Natural Resources and the Environment is gratefully acknowledged. Enrique Lizarraga-Garcia is greatly thankful to the "Caja Madrid" Foundation for his postgraduate fellowship. This research used resources of the Oak Ridge Leadership Computing Facility at the Oak Ridge National Laboratory, which is supported by the Office of Science of the U.S. Department of Energy under Contract No. DE-AC05-00OR22725. The authors would also like to express their gratitude to Dr. Narayanan and Mr. Caviezel from ASCOMP for their support.

A. APPENDIX: CODE VALIDATION

Previously, TransAT® code has been validated using data from the literature for the Taylor bubble terminal velocity in inclined pipes, and its film thickness in vertical pipes. This section completes the validation: the bubble shape of case 7 is compared with experimental data from Nogueira et al. (2006a) (Figure 8), and the velocity vectors of case 5 with experimental PIV data from Bugg and Saad (2002) (Figure 9 through Figure 11).

In Figure 8, the bubble profile in the YZ-plane (where the z-axis is the vertical) overlaps with the bubble profile in the perpendicular XZ-plane, confirming an axisymmetric profile. Figure 9 shows the axial velocity component along the tube axis above the tip of the bubble on the left subfigure: note that the presence of the bubble does not affect the flow beyond one diameter ahead of its tip. The axial and radial velocity components at $z/R = 0{,}222$ above the bubble tip are shown on the right subfigure. The axial velocity is positive in the center region of the pipe, and becomes negative in the periphery due to the suction of the film around the Taylor bubble. The radial velocity is zero at the tube axis due to symmetry and at $z/R = 1$ due to the tube wall, and is positive elsewhere since liquid is moving from the center region towards the pipe wall where it is suctioned by the liquid film. Figure 10 shows the axial and radial velocity components in the film transition region at $z/R = 1{,}008$ below the bubble nose on the left subfigure. The film is still developing since the radial velocity is not zero there. The axial velocity is negative in the whole film region. PIV particles are only observed in the liquid region, and the absence of them indicates the presence of the gas phase. The right subfigure of Figure 10 shows the axial velocity profile in the fully developed falling film at a distance $z/R = 4{,}64$ from the bubble nose. In this fully developed region, the radial velocity is zero as expected. Finally, Figure 11 depicts the axial and radial velocity components in the wake of the bubble at a distance $z/R = 0{,}4$ below the bubble tail. The radial velocity is negative since the liquid coming from the falling film at the pipe wall moves towards the pipe inner core. Furthermore, the axial velocity is positive in the inner core, and negative in the outer core due to the falling film, a characteristic of the recirculation taking place in this case's bubble wake. The comparison is successful and provides confidence in the use of TransAT® in this study.

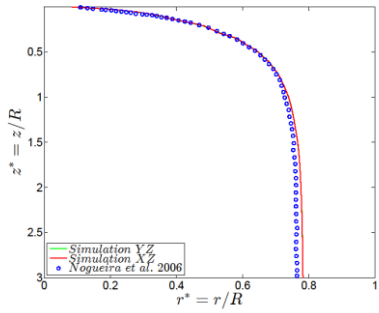

Figure 8: The Taylor bubble shape of case 7 obtained numerically is compared with the experimental results from Nogueira et al. (2006a).

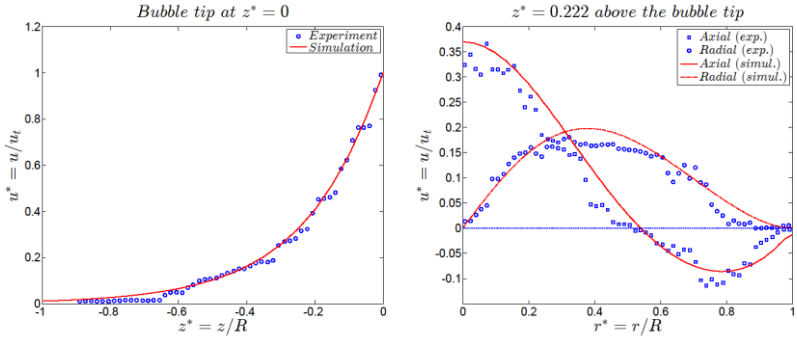

Figure 9: The velocity profile of case 5 ahead of the bubble in the pipe centerline (left) and across the radial axis (right) obtained numerically is compared with the experimental data of Bugg and Saad (2002).

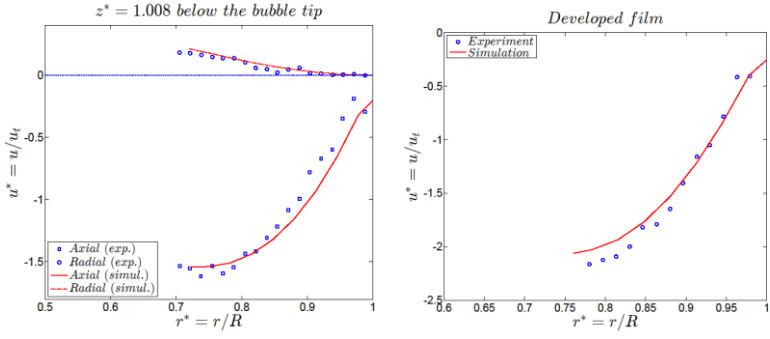

Figure 10: The velocity profile of case 5 in the developing region of the falling film (left) and in the developed film (right) obtained numerically is compared with the experimental data of Bugg and Saad (2002).

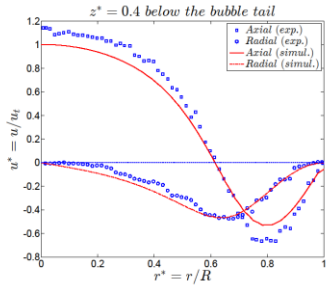

Figure 11: The velocity profile of case 5 in the wake of the bubble along the radial axis obtained numerically compared with the experimental data of Bugg and Saad (2002).

REFERENCES

Al-Safran, E. M., B. Gokcal, C. Sarica, and others, 2013, Investigation and Prediction of High-Viscosity Liquid Effect on Two-Phase Slug Length in Horizontal Pipelines: SPE Production & Operations, v. 28, p. 296-305.

Alves, I. N., O. Shoham, and Y. Taitel, 1993, Drift velocity of elongated bubbles in inclined pipes: Chemical engineering science, v. 48, p. 3063-3070.

Ansari, A. M., N. D. Sylvester, C. Sarica, O. Shoham, and J. P. Brill, 1994, A Comprehensive Mechanistic Model for Upward Two-Phase Flow in Wellbores: SPE Production and Facilities, v. 9, p. 143 - 151.

Araújo, J., J. Miranda, and J. Campos, 2013a, Flow of two consecutive Taylor bubbles through a vertical column of stagnant liquid—A CFD study about the influence of the leading bubble on the hydrodynamics of the trailing one: Chemical Engineering Science, v. 97, p. 16-33.

Araújo, J., J. Miranda, and J. Campos, 2013b, Simulation of slug flow systems under laminar regime: Hydrodynamics with individual and a pair of consecutive Taylor bubbles: Journal of Petroleum Science and Engineering, v. 111, p. 1-14.

Araújo, J. D. P., J. M. Miranda, A. M. F. R. Pinto, and J. B. L. M. Campos, 2012, Wide-ranging survey on the laminar flow of individual Taylor bubbles rising through stagnant Newtonian liquids: International Journal of Multiphase Flow, v. 43, p. 131 - 148.

Ben-Mansour, R., A. Sharma, B. Jeyachandra, B. Gokcal, A. Al-Sarkhi, and C. Sarica, 2010, Effect of pipe diameter and high oil viscosity on drift velocity for horizontal pipes: 7th North American Conference on Multiphase Technology, p. 237-248.

Bendiksen, K. H., 1984, An experimental investigation of the motion of long bubbles in inclined tubes: International journal of multiphase flow, v. 10, p. 467-483.

Bendiksen, K. H., D. Malnes, and O. J. O. NYDAL, RGEN, 1996, On the modelling of slug flow: Chemical Engineering Communications, v. 141, p. 71-102.

Bonnecaze, R. H., W. Erskine, and E. J. Greskovich, 1971, Holdup and pressure drop for two-phase slug flow in inclined pipelines: AIChE Journal, v. 17, p. 1109-1113.

Brill, J. P., and H. Mukherjee, 1999, Multiphase Flow in Wells: Monograph Vol. 17, SPE Henry L. Dogorty Series.

Bugg, J. D., K. Mack, and K. S. Rezkallah, 1998, A numerical model of Taylor bubbles rising through stagnant liquids in vertical tubes: International Journal of Multiphase Flow, v. 24, p. 271-281.

Bugg, J. D., and G. A. Saad, 2002, The velocity field around a Taylor bubble rising in a stagnant viscous fluid: numerical and experimental results: International Journal of Multiphase Flow, v. 28, p. 791-803.

Carew, P., N. Thomas, and A. Johnson, 1995, A physically based correlation for the effects of power law rheology and inclination on slug bubble rise velocity: International Journal of Multiphase Flow, v. 21, p. 1091-1106.

Caviezel, D., M. Labois, C. Narayanan, and D. Lakehal, 2013, Highly resolved multiphase flow topology in vertical pipes and risers: ICMF 2013 - 8th International Conference on Multiphase Flow.

Clarke, A., and R. Issa, 1997, A numerical model of slug flow in vertical tubes: Computers & fluids, v. 26, p. 395-415.

Collins, R., F. De Moraes, J. Davidson, and D. Harrison, 1978, The motion of a large gas bubble rising through liquid flowing in a tube: J. Fluid Mech, v. 89, p. 497-514.

Davies, R., and G. Taylor, 1950, The mechanics of large bubbles rising through extended liquids and through liquids in tubes: Proceedings of the Royal Society of London. Series A. Mathematical and Physical Sciences, v. 200, p. 375-390.

Dukler, A. E., and M. G. Hubbard, 1975, A model for gas-liquid slug flow in horizontal and near horizontal tubes: Industrial & Engineering Chemistry Fundamentals, v. 14, p. 337-347.

Dumitrescu, D. T., 1943, Stromung an einer Luftblase im senkrechten Rohr: ZAMM-Journal of Applied Mathematics and Mechanics/Zeitschrift für Angewandte Mathematik und Mechanik, v. 23, p. 139-149.

Fabre, J., and Liné, A, 1992, Modeling of two-phase slug flow: Annual Review of Fluid Mechanics, v. 24, p. 21-46.

Fréchou, D., 1986, Etude de l'écoulement ascendant à trois fluides en conduite verticale: Thèse Inst Natl Polythech, Toulouse, France.

Griffith, P., and G. B. Wallis, 1961, Two-Phase Slug Flow: Journal of Heat Transfer, v. 83.

Ha-Ngoc, H., and J. Fabre, 2004a, Test-case number 29a: The velocity and shape of 2D long bubbles in inclined channels or in vertical tubes (PA, PN). Part I: in a stagnant liquid.

Ha-Ngoc, H., and J. Fabre, 2004b, Test-case number 29b: The velocity and shape of 2D long bubbles in inclined channels or in vertical tubes (PA, PN). Part II: in a flowing liquid.

Hasan, A., and C. Kabir, 1988, Predicting Multiphase Flow Behavior in a Deviated Well: SPEPE, v. 3, p. 474-482.

Jeyachandra, B. C., B. Gokcal, A. Al-Sarkhi, C. Sarica, and A. Sharma, 2012, Drift-Velocity Closure Relationships for Slug Two-Phase High-Viscosity Oil Flow in Pipes: SPE Journal, v. 17, p. 593-601.

Kang, C.-W., S. Quan, and J. Lou, 2010, Numerical study of a Taylor bubble rising in stagnant liquids: Phys. Rev. E, v. 81, p. 066308.

Lakehal, D., D. Caviezel, C. Narayanan, M. Labois, S. Thomas, and others, 2012, Advanced Two-And Three-dimensional Simulation of Multiphase Flow In Horizontal And Vertical Pipes: 8th North American Conference on Multiphase Technology.

Lakehal, D., M. Labois, D. Caviezel, and B. Belhouachi, 2011, Transition of gas-liquid stratified flow in oil transport pipes: The Journal of Engineering Research, v. 8, p. 49-58.

Liu, Y.-P., P.-Y. Wang, J. Wang, and Z.-H. Du, 2013, Investigation of Taylor bubble wake structure in liquid nitrogen by PIV technique: Cryogenics, v. 55, p. 20-29.

Llewellin, E. W., E. D. Bello, J. Taddeucci, P. Scarlato, and S. J. Lane, 2012, The thickness of the falling film of liquid around a Taylor bubble: Proceedings of

the Royal Society A: Mathematical, Physical and Engineering Science, v. 468, p. 1041-1064.
Maneri, C. C., and N. Zuber, 1974, An experimental study of plane bubbles rising at inclination: International Journal of Multiphase Flow, v. 1, p. 623-645.
Mao, Z.-S., and A. Dukler, 1989, An experimental study of gas-liquid slug flow: Experiments in Fluids, v. 8, p. 169-182.
Mao, Z.-S., and A. E. Dukler, 1990, The motion of Taylor bubbles in vertical tubes. I. A numerical simulation for the shape and rise velocity of Taylor bubbles in stagnant and flowing liquid: Journal of Computational Physics, v. 91, p. 132 - 160.
Mao, Z.-S., and A. E. Dukler, 1991, The motion of Taylor bubbles in vertical tubes--II. Experimental data and simulations for laminar and turbulent flow: Chemical Engineering Science, v. 46, p. 2055 - 2064.
Nicklin, D., J. Wilkes, and J. Davidson, 1962, Two-phase flow in vertical tubes: Trans. Inst. Chem. Eng, v. 40, p. 61-68.
Nogueira, S., M. L. Riethmuler, J. B. L. M. Campos, and A. M. F. R. Pinto, 2006a, Flow in the nose region and annular film around a Taylor bubble rising through vertical columns of stagnant and flowing Newtonian liquids: Chemical Engineering Science, v. 61, p. 845 - 857.
Nogueira, S., M. Riethmuller, J. Campos, and A. Pinto, 2006b, Flow patterns in the wake of a Taylor bubble rising through vertical columns of stagnant and flowing Newtonian liquids: An experimental study: Chemical engineering science, v. 61, p. 7199-7212.
Orell, A., and R. Rembrand, 1986, A model for gas-liquid slug flow in a vertical tube: Industrial & engineering chemistry fundamentals, v. 25, p. 196-206.
Osher, S., and J. A. Sethian, 1988, Fronts propagating with curvature-dependent speed: algorithms based on Hamilton-Jacobi formulations: Journal of computational physics, v. 79, p. 12-49.
Petalas, N., and K. Aziz, 2000, A Mechanistic Model for Multiphase Flow in Pipes: Journal of Canadian Petroleum Technology, v. 39.
Polonsky, S., L. Shemer, and D. Barnea, 1999, The relation between the Taylor bubble motion and the velocity field ahead of it: International Journal of Multiphase Flow, v. 25, p. 957-975.
Shosho, C. E., and M. E. Ryan, 2001, An experimental study of the motion of long bubbles in inclined tubes: Chemical engineering science, v. 56, p. 2191-2204.
Spedding, P. L., and V. T. Nguyen, 1978, Bubble rise and liquid content in horizontal and inclined tubes: Chemical Engineering Science, v. 33, p. 987-994.
Stanislav, J. F., S. Kokal, and M. K. Nicholson, 1986, Intermittent gas-liquid flow in upward inclined pipes: International journal of multiphase flow, v. 12, p. 325-335.
Taha, T., and Z. F. Cui, 2006, CFD modelling of slug flow in vertical tubes: Chemical Engineering Science, v. 61, p. 676-687.
Taitel, Y., and D. Barnea, 1990, Two-phase slug flow: Advances in heat transfer, v. 20, p. 83-132.
Tomiyama, A., Y. Nakahara, and G. Morita, 2001, Rising velocities and shapes of single bubbles in vertical pipes: International Conference of Multiphase Flow, p. 1-12.
TransAT®, 2014, version 5.1.1: Zurich, Switzerland, ASCOMP GmbH.
Viana, F., R. Pardo, R. Yanez, J. L. Trallero, and D. D. Joseph, 2003, Universal correlation for the rise velocity of long gas bubbles in round pipes: Journal of Fluid Mechanics, v. 494, p. 379-398.
Wallis, G. B., 1969, One-Dimensional Two-Phase Flow, v. 1, McGraw-Hill New York.

Weber, M. E., A. Alarie, and M. E. Ryan, 1986, Velocities of extended bubbles in inclined tubes: Chemical engineering science, v. 41, p. 2235-2240.

White, E. T., and R. H. Beardmore, 1962, The velocity of rise of single cylindrical air bubbles through liquids contained in vertical tubes: Chemical Engineering Science, v. 17, p. 351-361.

Zukoski, E. E., 1966, Influence of viscosity, surface tension, and inclination angle on motion of long bubbles in closed tubes: Journal of Fluid Mechanics, v. 25, p. 821-837.